



Cholesterol synthesis inhibition promotes axonal regeneration in the injured central nervous system

Alireza P. Shabanzadeh^{a,b,c}, Jason Charish^{a,f}, Nardos G. Tassew^{a,b}, Nahal Farhani^a, Jinzhou Feng^e, Xijue Qin^e, Shuzo Sugita^a, Andrea J. Mothe^a, Thomas Wälchli^a, Paulo D. Koeberle^c, Philippe P. Monnier^{a,b,d,f,*}

^a Krembil Research Institute, KDT 8-417, 60 Leonard St., Toronto M5T 2S8, Ontario, Canada

^b Department of Physiology, Donald K. Johnson Research Institute, 60 Leonard St., Toronto M5T 2S8, Ontario, Canada

^c Department of Anatomy, Faculty of Medicine, University of Toronto, Toronto M5S 1A8, Ontario, Canada

^d Department of Ophthalmology, Faculty of Medicine, University of Toronto, Toronto M5S 1A8, Ontario, Canada

^e Department of Neurology, The First Affiliated Hospital of Chongqing Medical University, Chongqing 400016, China

^f Department of Physiology, Faculty of Medicine, University of Toronto, Toronto M5S 1A8, Ontario, Canada

ARTICLE INFO

Keywords:

Cholesterol inhibition
Axonal regeneration
Neuronal survival

ABSTRACT

Neuronal regeneration in the injured central nervous system is hampered by multiple extracellular proteins. These proteins exert their inhibitory action through interactions with receptors that are located in cholesterol rich compartments of the membrane termed lipid rafts. Here we show that cholesterol-synthesis inhibition prevents the association of the Neogenin receptor with lipid rafts. Furthermore, we show that cholesterol-synthesis inhibition enhances axonal growth both on inhibitory -myelin and -RGMa substrates. Following optic nerve injury, lowering cholesterol synthesis with both drugs and siRNA-strategies allows for robust axonal regeneration and promotes neuronal survival. Cholesterol inhibition also enhanced photoreceptor survival in a model of Retinitis Pigmentosa. Our data reveal that Lovastatin leads to several opposing effects on regenerating axons: cholesterol synthesis inhibition promotes regeneration whereas altered prenylation impairs regeneration. We also show that the lactone prodrug form of lovastatin has differing effects on regeneration when compared to the ring-open hydroxy-acid form. Thus the association of cell surface receptors with lipid rafts contributes to axonal regeneration inhibition, and blocking cholesterol synthesis provides a potential therapeutic approach to promote neuronal regeneration and survival in the diseased Central Nervous System.

Significance statement: Statins have been intensively used to treat high levels of cholesterol in humans. However, the effect of cholesterol inhibition in both the healthy and the diseased brain remains controversial. In particular, it is unclear whether cholesterol inhibition with statins can promote regeneration and survival following injuries. Here we show that late stage cholesterol inhibition promotes robust axonal regeneration following optic nerve injury. We identified distinct mechanisms of action for activated vs non-activated Lovastatin that may account for discrepancies found in the literature. We show that late stage cholesterol synthesis inhibition alters Neogenin association with lipid rafts, thereby i) neutralizing the inhibitory function of its ligand and ii) offering a novel opportunity to promote CNS regeneration and survival following injuries.

1. Introduction

When CNS axons are injured they do not regenerate, resulting in severe and persistent functional deficits (Schwab et al., 2005a; Hata et al., 2006). The inability of CNS axons to regenerate is largely associated with molecular aspects of the CNS environment that are inhibitory to axonal elongation. Following injuries, regenerating axons are

confronted with inhibitors present both in the glial scar and the myelin. For instance, CNS myelin contains extracellular proteins such as Nogo, MAG, RGMa and OMgp which work as contact dependent inhibitors for axons (McKerracher et al., 1994; Schwab, 2004; Wang et al., 2002). The glial scar contains another set of inhibitory proteins, including Chondroitin Sulfate Proteoglycans (CSPGs) and RGMa, that represent a barrier between the injured and healthy tissue (Buss et al., 2009; Monnier

* Corresponding author at: Krembil Research Institute, 60 Leonard Street, KDT 8-428, Toronto, ON M5T 2S8, Canada.

E-mail address: philippe.monnier@uhnresearch.ca (P.P. Monnier).

<https://doi.org/10.1016/j.nbd.2021.105259>

Received 7 August 2020; Received in revised form 24 December 2020; Accepted 7 January 2021

Available online 9 January 2021

0969-9961/© 2021 The Author(s).

Published by Elsevier Inc.

This is an open access article under the CC BY-NC-ND license

(<http://creativecommons.org/licenses/by-nc-nd/4.0/>).

et al., 2003(Hata et al., 2006)). Traumatic brain injury, spinal cord lesion, and ischemia all caused accumulation of these inhibitory molecules in lesion and peri-lesional areas (Schwab et al., 2005a; Schwab et al., 2005b). Thus, there is a large palette of extracellular factors that potentially account for the lack of regeneration in the injured CNS. There is strong evidence that regeneration can be achieved by blocking these inhibitory components, with neutralizing antibodies against RGMA and Nogo having been shown to restore some motor functions following spinal cord injury (Liebscher et al., 2005; Mothe et al., 2017; Hata et al., 2006). Neutralization of extracellular inhibitors of regeneration has therapeutic potential and further works aimed at identifying novel means of neutralization are therefore warranted.

The plasma membrane of injured neurons contains a combination of lipids and transmembrane receptors structured in glycolipoprotein microdomains called lipid rafts (Thomas et al., 2004). An important difference between lipid rafts and other membrane compartments is that lipid rafts contain larger amounts of cholesterol than the adjacent lipid-bilayer (Thomas et al., 2004). We and others have shown that lipid rafts contain the receptors for several of the inhibitory ligands that hamper regeneration. For instance, lipid rafts contain Neogenin and NgR, which are the receptors for RGMA and Nogo, respectively (Tassew et al., 2014; Yu et al., 2004). Signaling through Neogenin and NgR depends on their presence in lipid rafts, and cholesterol removal using the chemical chelator M β CD enhances axonal growth on RGMA and Nogo (Tassew et al., 2014; Yu et al., 2004). Lipid raft removal by the means of M β CD has furthermore been shown to promote regeneration and functional recovery in both the injured CNS and PNS, highlighting the potential of cholesterol removal to treat neuronal injuries (Rosello-Busquets et al., 2019; Tassew et al., 2014).

Under physiological conditions, plasma lipoproteins do not cross the blood brain barrier and the cholesterol found in the brain is synthesized in situ (Dietschy and Turley, 2001). Thus, brain cells depend on HMG-CoA reductase to produce their own cholesterol. Cholesterol synthesis inhibition by the means of statins has been widely used to lower blood cholesterol levels and reduce risk for illnesses related to atherosclerosis (Fulcher et al., 2015). Statins reduce cholesterol production by targeting the enzyme *HMG-CoA reductase*, and may or may not cross the blood brain barrier. Among the statins, some are largely excluded from the brain because they are water-soluble, while others that are fat-soluble can enter at least to some degree (Guillot et al., 1993). A recent screen identified statins as potent agents capable of promoting axonal regeneration in the injured CNS (Li et al., 2016). However, this study suggested that statins promote regeneration by inhibiting protein prenylation and not by altering cholesterol synthesis.

Here, we assessed the role of cholesterol inhibition on axonal regeneration and neuronal survival. We show that cholesterol synthesis-inhibition alters Neogenin recruitment into lipid rafts. Using drugs and small interfering RNA (siRNA) strategies, we show that preventing cholesterol synthesis i) promotes retinal ganglion cell survival and axonal regeneration following optic nerve injury and ii) promotes the survival of photoreceptors in an animal model of inherited retinal degeneration. Moreover, we show that cholesterol inhibition and prenylation can have opposing actions on regenerating axons.

2. Materials and methods

2.1. Small molecular drugs and chemical substances

AY9944 (Trans-N, N-bis [2-Chlorophenylmethyl]-1, 4-cyclohexanedimethanamine dihydrochloride, CAT#1639, Tocris Bioscience, ON, Canada). Lovastatin (CAT#1530, Tocris Bioscience, ON, Canada). GGPP (Geranylgeranyl pyrophosphate ammonium salt, G6025, Sigma-Aldrich, ON, Canada). BM15.766 (4-(2-[1-(4-chlorocinnamyl) piperazin-4-yl]ethyl)-benzoic acid; D7-reductase inhibitor (Tocris Bioscience, ON, Canada). Poly-L-Lysine (CAT: 26124-78-7; Sigma-Aldrich, ON, Canada).

2.2. Lovastatin activation protocol

10 mg of Lovastatin was dissolved in 250 μ l of 100% ethanol. 100 μ l of the solution was mixed with 150 μ l of 0.1 N NaOH for 2 h at 50 °C. pH was adjusted to 7–7.2 with HCL. ddH₂O was then added to the solution to make a final concentration of 4 mg/ml Lovastatin (Gerson et al., 1989; Sadeghi et al., 2000; Todd and Goa, 1990).

2.3. Chick retinal explant outgrowth assay on myelin and RGMA

Myelin was purified from rat spinal cords using sucrose fractionation as follows: approximately 10 g of rat spinal cord was homogenized in 0.25 M sucrose, pH 7.4, in a glass homogenizer with Teflon pestle. All operations are carried out at 4 °C. The volume was brought up to 10 ml with sucrose. The gradient was then introduced at the side using the gradient pump, gradually increasing the concentration of sucrose from 0.32 to 0.88 M. The sample was then spun at the 96,000 g. for 1 h. The material that floated on the 0.32 M-sucrose was collected. This fraction was diluted 4-fold with water and spun at 96,000 g for 30 min. The resulting pellet was resuspended in distilled water. BCA assay was used to measure the protein concentration and the myelin was aliquoted at 2 mg protein/ml.

RGMA protein was purified using Nickel-agarose as we described previously (Tassew et al., 2017). Following purification the protein was dialyzed against PBS and stored at –80 °C.

Retinal explants were performed as previously described (Tassew et al., 2017; Tassew et al., 2014). Retinal explants were prepared from E7 chick embryos and cultured on coverslips coated with Laminin (Invitrogen; 10 μ g/ml), Laminin plus RGMA (10 μ g/ml), and Laminin plus myelin (50 μ g/ml), and treated with control (0.1% DMSO), AY9944 (1 μ M), BM15.766 (4 μ M), activated Lovastatin (A-Lova; 12.5 μ M), and A-Lova (12.5 μ M) plus GGPP (10 μ M). After 18 h in culture, explants were fixed with 4% PFA and stained with Alexa 488-Phalloidin (Molecular Probes; 1:50). Neurite length was measured using CellSens software. At least three independent experiments were done and data is presented as mean \pm SEM.

2.4. Chick retinal explant outgrowth assay on RGMA

Poly-L-Lysine (10 μ g/ml) coated glass coverslips were treated with Laminin (10 μ g/ml) or Laminin plus RGMA (5 μ g/ml) and incubated for 3 h. at room temperature. Retinal explants were treated with control (0.1% DMSO), A-Lova (12.5 μ M), non-activated Lovastatin (NA-Lova; 12.5 μ M), GGPP (10 μ M), A-Lova (12.5 μ M) plus GGPP (10 μ M), and NA-Lova (12.5 μ M) plus GGPP (10 μ M). Fixation, staining and neurite measurements were performed as described above. Data is presented as mean \pm SEM.

2.5. Lipid raft fractionation of chicken brain and western blots

Chick E8 tecta (3 tecta for each set of experiments) were injected with PBS + 0.1%DMSO (Control), PBS + AY9944 (25 μ M), PBS + A-Lova (6.5 μ M), PBS+ A-Lova (6.5 μ M) + GGPP (3.1 μ g/ml) and collected 24 h later. Tecta were lysed and placed at the bottom of a sucrose density gradient (0.9–0.8–0.75–0.7–0.6–0.5–0.4–0.2 M) and centrifuged at 38,000 rpm for 16 h in an SW 60 rotor (Beckman Instruments Inc.). After centrifugation 200 μ l samples were collected (numbered 1 to 8 beginning at the top) and used in western blotting analysis. Primary antibodies consisted of: rabbit-anti-Neogenin (1:500; H-175, Santa Cruz); goat-anti-flotillin-1 (1:500; C-20, Santa Cruz) and mouse-anti-transferrin receptor (1:500; CD71, Santa Cruz). Odyssey secondary antibodies (1:10000; LI-COR) were incubated 1 h at room temperature.

2.6. Validation of DHCR7 siRNA knockdowns

N1E-115 neuroblastoma cells were cultured as described (Molenaar et al., 2008; Vreugdenhil et al., 2007). For microscopy, N1E-115 cells were grown in 24-well plates with glass bottom (Greiner Bio-One, NY, USA) coated with 200 ng/ml Poly-L-lysine at 80% confluence. N1E-115 neuroblastoma cells were transfected with 50 nM DHCR7 siRNA (for 48 h) using lipofectamine 2000 (Invitrogen) as described in the manufacturer's protocol. Control #1 siRNA (AM4611) from Life Technologies Inc. was used as negative control. A transfection efficiency of $95 \pm 5\%$ was obtained, which was determined by quantifying the percentage of transfected cells with a non-targeting siRNA conjugated to FITC.

The lysates were run on western blots and probed with rabbit-anti-DHCR7 (1:1000; ThermoFisher Scientific; IL, USA). An IR-Odyssey secondary antibody (1:10000; LI-COR) was incubated for 1 h at room temperature. For quantification, the optical density of each band was normalized against the density of the corresponding beta-actin band for each lane. The normalized densitometry values for each experimental group were reported as mean \pm SEM.

2.7. Optic nerve crush

Adult male Sprague Dawley rats (Charles River, Senneville, QC, Canada), weighing 250–300 g, were kept in a pathogen free environment and cared for according to guidelines from the Canadian Council on Animal Care. Optic nerve crush was performed as we have previously described (Magharious et al., 2011a; Magharious et al., 2011b; Shabanzadeh et al., 2019). One week prior to surgery, animals received stereotaxic injections of 2% Fluorogold into the superior colliculus in order to target retinal ganglion cells (RGCs). Animals were placed in a stereotaxic frame and anesthetized with isoflurane (2%; 0.8 l/min oxygen flow rate). The optic nerve was accessed within the ocular orbit via an incision in the tissue covering the superior border of the orbital bone. The optic nerve was crushed within 2 mm of the back of the eye, for 6 s using fine self-closing forceps. The meningeal coverings of optic nerve remained intact.

2.8. Medications and injection protocol

In order to evaluate the effects of A-Lova, A-Lova plus GGPP, and AY9944 on RGC survival, intraretinal axon integrity, and axon regeneration after optic nerve crush, animal were randomized and divided into separate groups ($n = 7$ each). For each group, animals received intravitreal injections at 3 and 10 days post optic nerve crush. The groups consisted of the following: i) a control group that received intraocular injection of DMSO vehicle, ii) a treatment group that received intraocular injections of A-Lova (10 μ M), iii) a treatment group receiving injections of A-Lova (10 μ M) plus GGPP (3.1 μ g/ml) and iv) a treatment group that received intraocular injections of AY9944 (5 μ M) solutions. Intraocular injections were described previously (Magharious et al., 2011b; Magharious et al., 2011c). Briefly, the rats were initially anesthetized with 2% isoflurane in a mix of O₂ and then the cornea was anesthetized using Alcaine eye drops (Alcon) prior to intraocular injections. A pulled glass micropipette attached to a 10 μ l Hamilton syringe via a hydraulic coupling through PEEK tubing was used to deliver solutions into the vitreous chamber of the eye, posterior to the limbus.

For experiments in rd1 mice, as above mice were given intraocular injections of AY9944, A-Lova, A-Lova + GGPP or control (DMSO in PBS), except here injections were performed using a 10 μ l gastight Hamilton syringe equipped with a blunt end 32G 0.5 in. tip. One drop of Alcaine and one drop of mydriatic agent were applied to the eyes of anesthetized mice prior to injection. A 30G needle was used to create an opening in the sclera at the limbus. The blunt end needle tip was gently inserted into the vitreous until observable through the lens, with care taken to avoid contact with the surrounding retina and lens. 1 μ l of solution was slowly injected into the vitreous. If there was any indication of lens injury, retinal detachment or bleeding with the eye, the sample was

excluded from subsequent analysis. Injections were performed at post-natal day (P)9 and P15 and eyes were harvested at P21.

2.9. Outer nuclear layer thickness quantification

Prior to harvesting at P21, the nasal quadrant of the eye was marked using a silver nitrate stick. Eyes were fixed in 4% PFA in PBS for 1 h, washed in PBS, then placed in 30% sucrose in PBS overnight. 14 μ m cryosections were generated throughout the entire retina, though only cryosections from the central retina, containing the optic nerve, were used for thickness quantifications. The thickness and the number of rows of cells in the photoreceptor containing Outer Nuclear Layer (ONL) were measured at 400 μ m from the optic disc in the nasal and temporal quadrant of each eye and averaged. The ONL was identified using DAPI nuclear stain.

2.10. DHCR7 siRNA treatments after optic nerve crush

To test the effect of siRNA treatment after optic nerve crush on RGC survival in the retina, animals were randomized into two groups ($n = 7$ each): a control group that received intraocular injections of Negative control siRNA (AM4611; Negative control No. 1 siRNA) and a test group that received optic nerve crush surgery followed by intraocular injections of DHCR7 siRNA (AM16708, Silencer pre-designed siRNA). All siRNAs used in this study were synthesized by Life Technologies Inc. (Burlington, ON, Canada). The following DHCR7 siRNA duplex sequences were used in the present study:

Sense: 5'-GGCCAUUGAGUGCUCCUACtt-3'; Antisense: 5'-GUAG-GAGCACUCAUUGGCtt-3'.

An intravitreal injection of 4 μ l of a 30 nmol solution of siRNA was administered per rat eye after optic nerve crush. The effect of control and DHCR7 siRNAs on regeneration was assessed by quantifying the number of Growth Associated Protein 43 (GAP43)-labeled axons (Anti-GAP-43; Cell Signaling Technology) at 21 days after in optic nerve injury.

2.11. Quantification of RGC survival after injury

RGC survival after injury was quantified via two different methods: Fluorogold retrograde labeling and immunohistochemistry directed against RNA-binding protein with multiple splicing (RBPMS) staining as previously detailed (Magharious et al., 2011a; Shabanzadeh et al., 2015; Tasew et al., 2017). Epifluorescence imaging was used to visualize Fluorogold pre-labeled RGCs after retinal ischemia. Following retrograde labeling with Fluorogold, RGC cell bodies in the ganglion cell layer and axon fascicles in the nerve fiber layer of the retina were clearly visible upon imaging in a flat mount preparation. Animals were euthanized at 21 days after optic nerve crush, at which point the eyes were enucleated, dissected, and the retinas fixed in 4% paraformaldehyde for 1 h and then rinsed in PBS for 15 min. The retinas were then flat-mounted and coverslipped in 50: 50 glycerol/PBS media for visualization. Fluorogold staining in RGCs was visualized with a fluorescence microscope using a wide band ultraviolet excitation filter and an Andor Neo sCMOS camera mounted on a Leica DM LFSA microscope. A Sutter Lambda XL illuminator (Quorum Technologies, Guelph, Canada) served as the light source with liquid light guide ensuring even field illumination. The density of RGCs was measured at three different distances from the central optic disk of the flat-mounted retinas: samples were taken from the inner (1/6 retinal eccentricity from the optic disk), mid-periphery (1/2 retinal eccentricity from the optic disk), and outer retina (5/6 retinal eccentricity from the optic disk) of the retinal quadrants. RGC densities (cells/mm²) were grouped by retinal eccentricity (inner, middle, outer) and expressed as mean \pm SEM.

RBPMS immunohistochemistry was performed on whole retinas. Iba-1 and GFAP immunohistochemistry was performed on retinal sections (12 μ m). Sections/Retinas were incubated overnight at 4 °C in an anti-

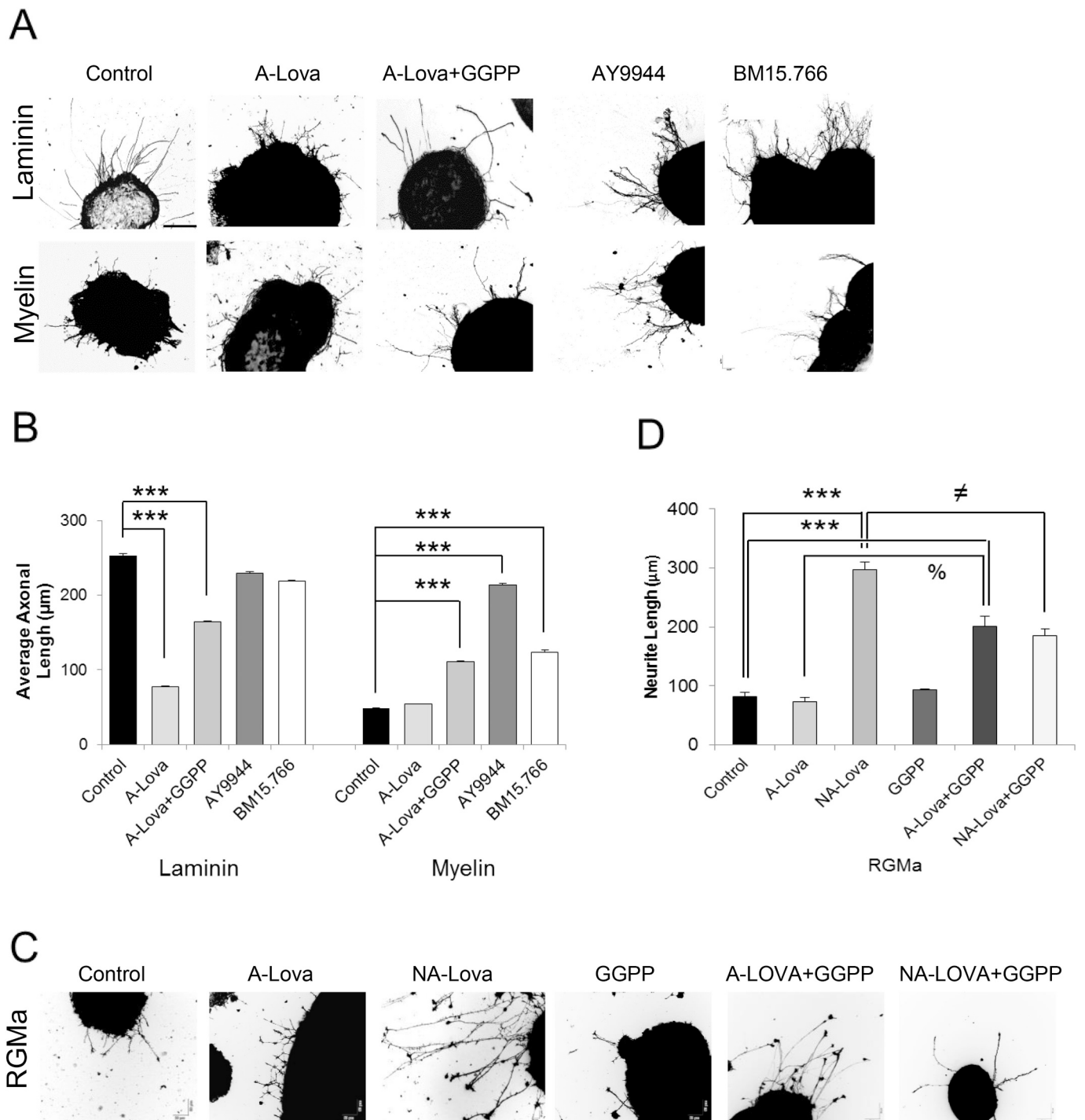


Fig. 1. Cholesterol synthesis inhibition promotes outgrowth on inhibitory proteins.

A, Retinal explants cultured on Laminin or myelin and treated with DMSO (0.1%, Control), activated Lovastatin (A-Lova) (12.5 μM), A-Lova (12.5 μM) + GGPP (10 μM), AY9944 (1 μM) and BM15.766 (4 μM). **B**, Quantification of axonal outgrowth on Laminin and myelin. **B (left)**, explants were grown on Laminin (Control), Laminin plus A-Lova + GGPP, AY9944, or BM15.766. **B (right)**, Explants were grown on myelin plus A-Lova + GGPP, AY9944, or BM15.766. **C**, Retinal explants cultured on Laminin plus RGMa and treated with DMSO (0.1%, Control), A-Lova (12.5 μM), non-activated Lovastatin (NA-Lova) (12.5 μM), GGPP (10 μM), a combination of A-Lova (12.5 μM) + GGPP (10 μM), and a combination of NA-Lova (12.5 μM) + GGPP (10 μM). **D**, Quantification of axonal outgrowth on Laminin plus RGMa, explants were grown on RGMa plus NA-Lova, a combination of A-Lova and GGPP, and a combination of NA-Lova and GGPP. Data are presented as mean \pm SEM ($n = 3$ independent experiments). *** $p < 0.0001$ vs. Control, % $p < 0.001$ vs. A-Lova, and # $p < 0.001$ vs. NA-Lova, Scale bars, 60 μm .

RBPMs (1: 500, PhosphoSolutions, Aurora, CO, USA), an anti-GFAP (1:500, Sigma-Aldrich, Mississauga, Ontario), or an anti-Iba-1 primary antibody (1:200, FujiFilm, Richmond, USA). The primary antibody was diluted in PBS containing 0.3% Triton X-100 and 3% normal serum. Following primary antibody incubation, retinas/sections were rinsed three times for 15 min in PBS and incubated with FITC/TRITC-labeled secondary antibody for 3 h at room temperature. Retinas were then rinsed three times for 15 min each time in PBS, flat mounted and coverslipped with 50: 50 glycerol/PBS. Epifluorescence imaging was used to visualize and quantify RGCs or glia cells.

2.12. Quantification of RGC axon regeneration

Retinal ganglion cell axon regeneration was assessed at 21 days after optic nerve crush as previously described (Monnier et al., 2011; Shabanzadeh et al., 2019). On day 21, animals were given an intracardial perfusion of PBS followed by 4% paraformaldehyde, and their optic nerves were carefully removed. Nerves were cryosectioned and immunohistochemistry using antibodies against GAP-43 (1:250; Cell Signaling Technology) were performed. GAP-43 is expressed in neuronal growth cones during development and axonal regeneration (Berry et al., 1996; Kuratomi et al., 2009), and is expressed by RGCs during axon outgrowth (Meiri et al., 1986; Schaden et al., 1994). Four equally spaced sections were examined across the width of each optic nerve. These were imaged using a Leica DM LFSa microscope (Leica Microsystems, Concord, Canada) with an Andor iXon 885 + camera (Andor Technology, Belfast, Northern Ireland). The total number of regenerating axons was quantified for each of the following distances from the crush site: 0–250 μm ; 250–500 μm ; >500 μm . The total number of regenerating axons at each distance was averaged and expressed as a mean \pm SEM. Statistical analysis was performed by ANOVA and Tukey's post hoc test.

2.13. Intraretinal axon integrity after optic nerve injury

Intraretinal axon integrity was assessed at 21 days after optic nerve crush as previously described (Monnier et al., 2011). Two days before removal of the nerve and fixation, the anterograde tracer FITC-conjugated cholera toxin B (CTB-FITC) was injected into the vitreous chamber of the eye to trace axons that were intact and capable of protein transport within the retina ($n = 7$, each group). At 21 days after optic nerve crush eyes were enucleated, dissected, and the retinas fixed in 4% paraformaldehyde for 1 h and then rinsed in PBS for 15 min. The retinas were then flat-mounted and coverslipped in 50: 50 glycerol/PBS media visualizing cholera toxin B (FITC conjugated). The integrity of axons was measured at three different distances from the central optic disk of the flat-mounted retinas: samples were taken from the inner (1/6 retinal eccentricity from the optic disk), mid- periphery (1/2 retinal eccentricity from the optic disk), and outer retina (5/6 retinal eccentricity from the optic disk) of the retinal quadrants. Axons integrity (axons/ mm^2) were grouped by retinal eccentricity (inner, middle, outer) and expressed as mean \pm SEM.

2.14. Cholesterol quantification

Cholesterol quantification was done using the Cholesterol/Cholesteryl Ester Quantification Assay kit (Abcam, ab65359). Briefly, chick tecta received a 3–4 μl injection of AY-9944 (25 μM); A-Lova (6.5 μM); or PBS. A day after injection, tecta were collected and 10 mg from each tecta was placed in an Eppendorf tube for cholesterol quantification. Lipids were extracted using 200 μl of Chloroform isopropanol NP-40 (7:11:0.1) in a micro homogenizer. Following centrifugation, the organic phase was collected air dried and re-suspended in 200 μl of Assay Buffer. Further development was performed according to the manufacturer's protocol.

2.15. Statistical analysis

The data for neurite outgrowth length, GAP-43 immunopositive axon growth numbers, CTB-FITC positive retinal axons, RGC densities (grouped by retinal eccentricity- inner, middle, outer), RBPMs immunopositive cells densities, and photoreceptor outer nuclear layer thicknesses were presented as mean \pm SEM. Statistical significance between groups was calculated by performing an analysis of variance (one-way ANOVA) followed by the Tukey's post hoc tests. For membrane fractionation western blots, normalized densitometry values for each experimental group were reported as mean \pm SEM, and statistically significant differences between experimental and control groups were calculated using an ANOVA followed by post hoc analysis using Tukey's post hoc comparisons. For DHCR7 siRNA's western blots, normalized densitometry values (relative to GFAP) for each experimental group and expressed as \pm SEM, and statistical analysis was performed by unpaired *t*-test. Differences were considered significant when $P < 0.05$. The variance is similar between the groups that are being statistically compared.

3. Results

3.1. Cholesterol synthesis inhibition promotes outgrowth on inhibitory proteins

A recent screen suggested that statins promote regeneration through inhibition of protein prenylation (Li et al., 2016). Because this study involved the screening of a large number of compounds, it can be assumed that the chemicals tested were not subjected to any specific activation procedure. Some statins (e.g. Lovastatin and Simvastatin) are lactone pro-drugs and are subsequently hydrolyzed in vivo to biologically active forms. In vitro, these statins require an activation step (e.g. hydrolysis with NaOH) prior to use (Keyomarsi et al., 1991; Ward et al., 2019). Here we reassess the potential impact of cholesterol inhibition on axonal outgrowth using both a statin (Lovastatin), as well as two late stage inhibitors of cholesterol synthesis (AY9944, and BM15.766) that act down-stream of statins (Honda et al., 1998; Igarashi et al., 1975). To do so, we first cultured retinal explants on a permissive growth substrate (Laminin). After 24 h in culture, axonal outgrowth on Laminin was impaired by addition of activated Lovastatin (A-Lova; 12.5 μM ; $77.47 \pm 1.25 \mu\text{m}$) when compared to control treated explants (0.1% DMSO; $252.32 \pm 2.78 \mu\text{m}$). These results suggests that A-Lova negatively affects outgrowth, however this may be independent from its action on cholesterol synthesis, given that 1 μM AY9944 ($228.82 \pm 2.97 \mu\text{m}$) or 4 μM BM15.766 ($218.35 \pm 1.12 \mu\text{m}$; Fig. 1A) failed to show a similar detrimental effect on outgrowth. Statins are inhibitors of HMG-CoA reductase which allows for the synthesis of Mevalonic acid, a precursor for both cholesterol and Geranylgeranyl Pyrophosphate (GGPP). GGPP is necessary for protein prenylation (Samuel and Hynds, 2010), something which is critical for the proper activity of axon-growth promoting proteins such as members of the Rho-GTPase family (Samuel and Hynds, 2010). Thus, we wondered whether axonal outgrowth inhibition by A-Lova was due to a reduction in GGPP synthesis. We tested this possibility by adding A-Lova (12.5 μM) plus GGPP (10 μM) to the medium, and observed a restoration of axonal growth to $\sim 75\%$ of control values on Laminin (Fig. 1B, left), indicating that A-Lova primarily alters axonal growth on laminin by reducing GGPP levels and protein prenylation.

Next, we assessed the role of cholesterol-synthesis inhibition on explant outgrowth on myelin, which is the main inhibitory component of the CNS. The mechanisms whereby myelin block axonal growth is believed to be conserved between species, hence we tested axonal growth of chick retinal neurons on rat myelin (Ng et al., 1996). On myelin, axonal growth was limited when compared to outgrowth on Laminin ($48.29 \pm 0.50 \mu\text{m}$; Fig. 1A). The addition of A-Lova to the medium did not affect outgrowth, which remained very poor ($53.91 \pm$

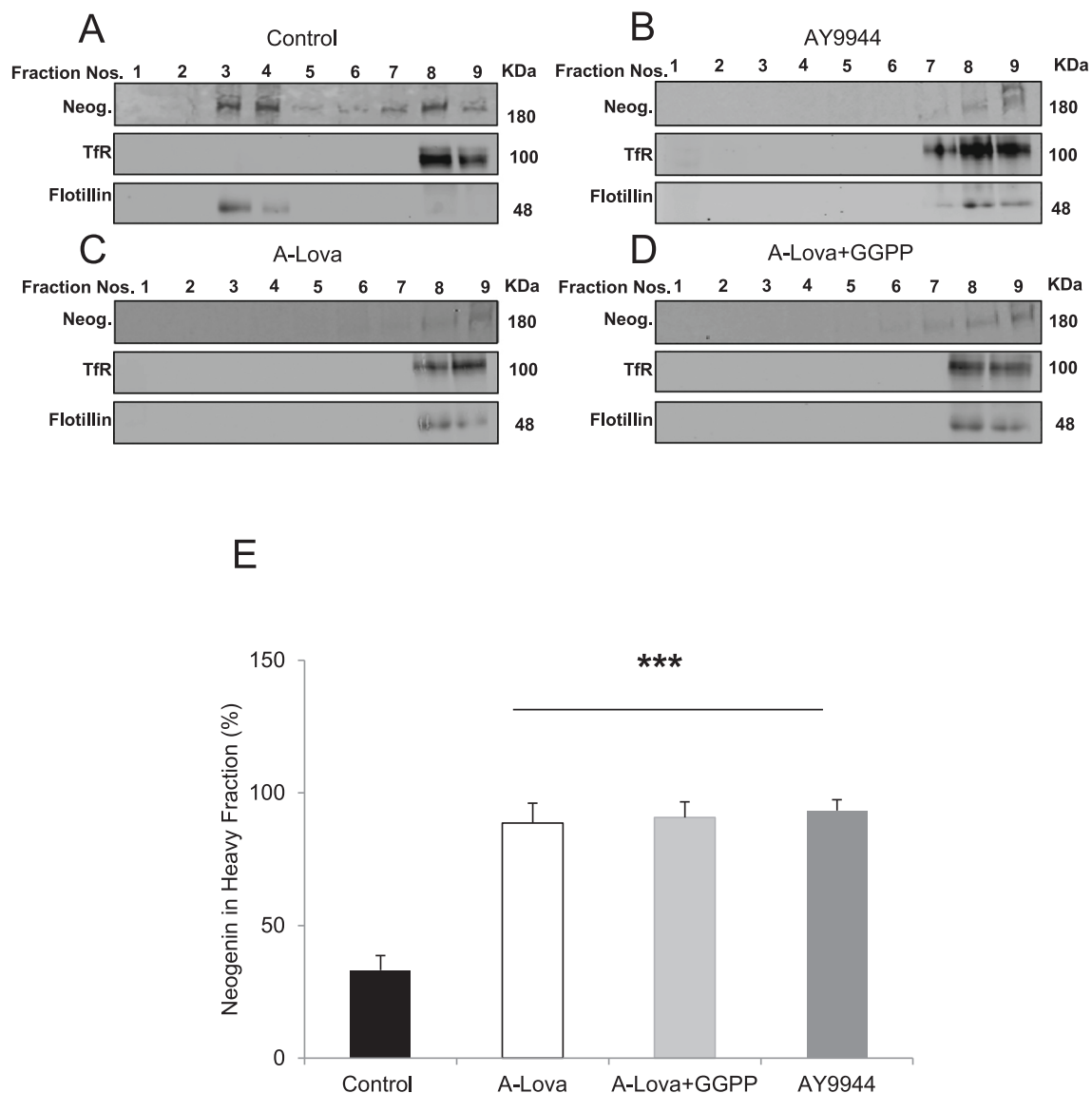


Fig. 2. Cholesterol synthesis inhibition disturbed the integrity of lipid rafts.

A-D, Western immunoblots and lipid raft fractionation of chick E8 midbrain lysates of **A**, control (PBS + 0.1%DMSO); **B**, PBS + AY9944 (25 μ M, 10 μ g/ μ l); **C**, PBS + A-Lova (6.5 μ M, 1 μ g/ μ l), and **D**, PBS+ A-Lova + GGPP (GGPP, 3.1 μ g/ml; A- Lova, 6.5 μ M). Chick brain gradient fractionation (top numbered 1 and next eight fractions numbered sequentially) showing that the majority of Neogenin co-localizes with raft marker Flotillin but not the heavy fraction marker Transferrin receptor (TfR). **E**, Graph depicting the mean normalized densitometry value (\pm SEM) of Neogenin in the heavy fraction of blots for each treatment. Treatments with either AY9944, A-Lova, or A-Lova+GGPP altered Neogenin localization. *** $p < 0.0001$ vs. Control. 3 tecta for each set of the experiment.

0.51 μ m; Fig. 1B, right). Interestingly, when either A-Lova (12.5 μ M) + GGPP (10 μ M) (111.05 \pm 0.90 μ m), AY9944 (213.70 \pm 2.09 μ m), or BM15.766 (123.056 \pm 3.52 μ m) were added to the medium, we observed a significant increase of axonal growth. Because GGPP on its own does not affect axonal growth (Supplementary Fig. 1), this suggests that cholesterol inhibition specifically can restore outgrowth on myelin (Fig. 1A and B).

The above presented data appear in contradiction with a previous study suggesting that blocking protein prenylation as opposed to cholesterol synthesis caused the outgrowth promoting effect of statins (Li et al., 2016). One potential difference between that study and ours may involve the activation status of the statins tested. We therefore compared the effect of non-activated Lovastatin (NA-Lova) and activated Lovastatin (A-Lova) on explants grown on the substrate RGMa, which is an inhibitory component of myelin (Schwab et al., 2005b; Zhang et al., 2011). Interestingly, NA-Lova significantly promoted axonal growth on RGMa compared to controls, whereas A-Lova did not

promote outgrowth on the inhibitory substrate (331.14 \pm 15.89 μ m for NA-Lova; 121.66 \pm 14.21 μ m for A-Lova; Fig. 1C and D). The mechanism by which NA-Lova promotes this outgrowth remains unknown, though the pro-drug lactone form of lovastatin can have various effects independent of HMGCoA (Muskal et al., 2016; Rao et al., 1999; Walther et al., 2016). Interestingly, the addition of GGPP to NA-Lova reduced the outgrowth promotion of NA-Lova, suggesting that under certain circumstances additional prenylation can act as a block on outgrowth (Li et al., 2016). However, it is important to note that the activated hydroxy acid form of lovastatin (A-Lova), which both lowers prenylation and cholesterol synthesis by acting through HMGCoA, inhibited outgrowth on laminin. In agreement with this inhibitory activity, A-lova activity on inhibitory substrate differed from that of NA-Lova as it did not promote outgrowth on RGMa or myelin (Fig. 1A–D). Here the addition of GGPP to A-Lova reduced the outgrowth inhibitory effect of A-Lova on laminin (Fig. 1), and led to the promotion of outgrowth on inhibitory substrates (Fig. 1 A–D), suggesting that in this context a

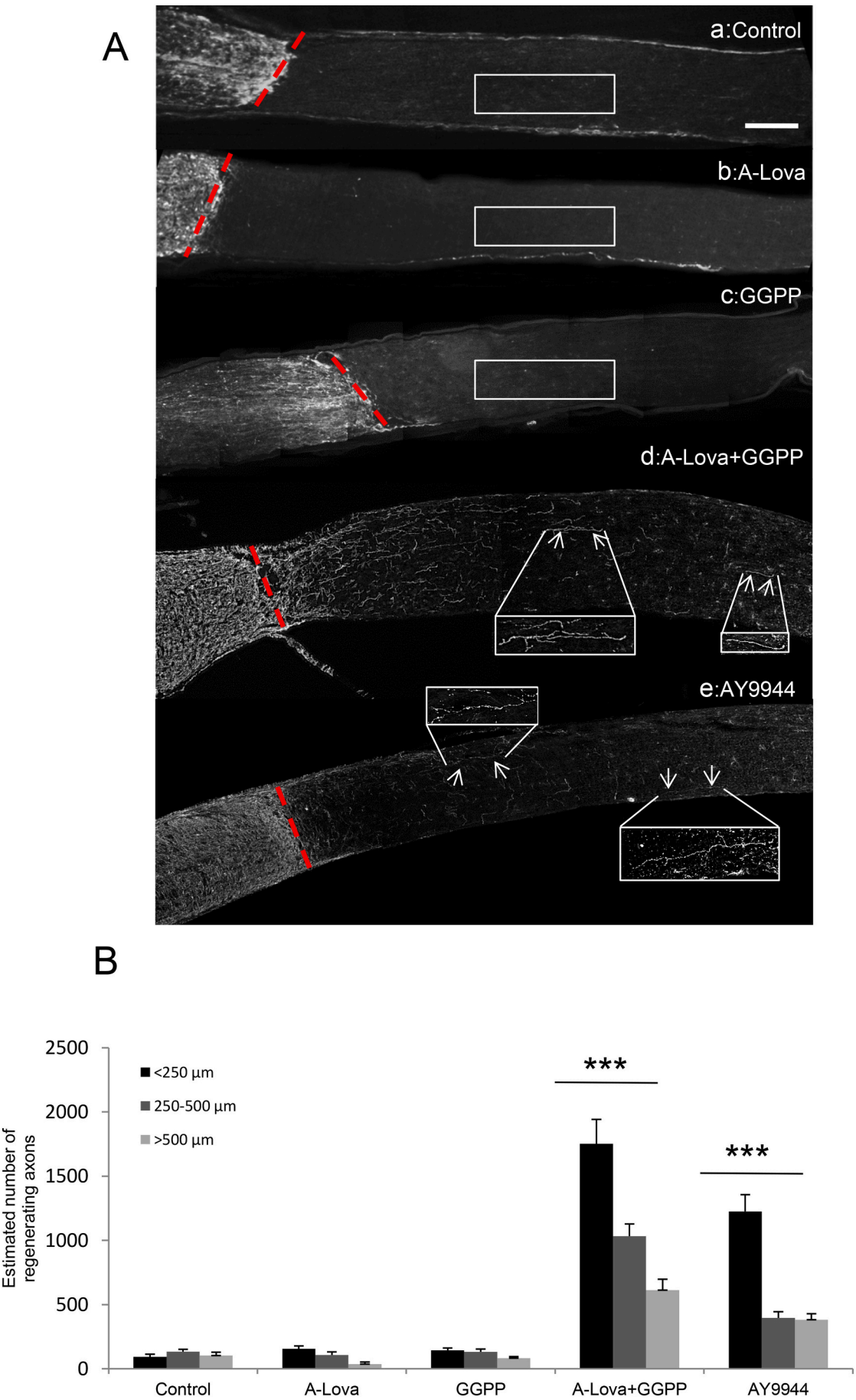


Fig. 3. Cholesterol inhibition with small molecular drugs enhance axonal regeneration after traumatic insult.

A, Epifluorescence micrographs of Growth Associated Protein 43 (GAP-43) -immunolabelled sections of optic nerves fixed at 21 days after optic nerve crush. Intraocular (IO) injections were delivered at 3- and 10 days following injury. Crush site is indicated by slanted dash line. Arrows demarcate some of the regenerating axons in each section. The retina (not visible) is towards the left-hand side of each image. **Aa,** Nerve that received vehicle IO treatment showed minimal axonal regeneration beyond the crush site. **Ab,** active Lovastatin (A-Lova)-treated nerves did not display the axonal regeneration when compared to control. **Ac,** GGPP treated animals did not display regeneration. **Ad-e,** Nerves treated with a combination of A-Lova plus Geranylgeranyl pyrophosphate (GGPP) or AY9944 showed enhanced axonal regeneration into the distal optic nerve. **B,** Quantification of the mean number of regenerating axons (\pm SEM) at 21 days following optic nerve crush. The number of axons was quantified in three bins distal to the crush site (0–250 μ m, 250–500 μ m, and > 500 μ m). The injections of a combination of A-Lova and GGPP or AY9944 significantly increased RGC axon regeneration compared to vehicle controls in the corresponding bin. *** P < 0.001 relative to control, scale bar, 200 μ m, n = 7 for each group.

(caption on next page)

reduction in prenylation was masking the growth promoting effect of A-Lova. AY9944 and BMI15766 also promoted outgrowth on an inhibitory substrate; this indicates that cholesterol synthesis inhibition itself promotes outgrowth.

3.2. Cholesterol synthesis inhibition abrogates the formation of lipid rafts

We have shown that the RGMa receptor Neogenin requires association with lipid rafts in order to be functional (Tassew et al., 2014). Furthermore, cholesterol depletion alters the formation of lipid rafts (Kim et al., 2009). In neurons, cholesterol is primarily derived from de novo synthesis (Dietschy and Turley, 2001). Cholesterol quantification confirmed that A-Lova and AY9944 reduced cholesterol levels in the CNS (Supplementary Fig. 2). We hypothesized that cholesterol inhibition restores outgrowth on RGMa by preventing Neogenin association with lipid rafts. To test this possibility, we treated chick brains with inhibitors of cholesterol synthesis *in ovo* and then subsequently performed membrane fractionations on the brains (Fig. 2A–E). In control (DMSO) treatments, we observed that the majority of Neogenin co-localized with a marker for lipid raft fractions (Flottilin) but not with a heavy membrane marker (TfR). As expected, treatments with either AY9944, A-Lova, or A-Lova + GGPP altered Neogenin localization. In the presence of cholesterol-synthesis inhibitors, both Neogenin and Flottilin-1 co-localized with TfR, suggesting the abrogation of lipid rafts (Fig. 2B–D). This argues that one mechanism by which cholesterol-synthesis inhibition promotes outgrowth on inhibitory molecules is by preventing membrane receptor activation into lipid rafts.

3.3. Cholesterol synthesis inhibition promotes regeneration in the injured CNS

These *in vitro* results suggest that segregating receptors (e.g. Neogenin) from lipid rafts supports axonal outgrowth on inhibitory proteins (e.g. RGMa, myelin). Furthermore, strategies that promote axonal growth of embryonic neurons on inhibitory myelin components have also promoted axonal regeneration in the injured CNS (Tassew et al., 2014, 2017). Hence, we wondered if the positive effect of cholesterol inhibition could be harnessed in order to promote neuronal regeneration in the injured adult mammalian CNS. To address this possibility, we studied regeneration following optic nerve injury in rats. Following injury, animals received intra-ocular injections of cholesterol synthesis inhibitors and axonal regeneration was examined 3 weeks later (Fig. 3Aa–Ae). Optic nerves were assessed using GAP-43 immunostaining in order to visualize regenerating adult RGC-axons (Meyer et al., 1994; Monnier et al., 2011). In controls, few axons extended beyond the lesion site within the optic nerve (Fig. 3A and B; <250 μ m: 92.57 ± 20.57 ; 250–500 μ m: 133.71 ± 18.77 ; and > 500 μ m: 102.85 ± 26.55). In contrast, animals treated with either A-Lova + GGPP or AY9944 displayed strong regeneration beyond the lesion site and pronounced axonal sprouting in the proximal segment of the nerve (Fig. 3Ad and 3Ae). Quantification of axon numbers by length showed that cholesterol inhibition significantly increased the number of regenerating axons by 8.05 fold relative to controls (Fig. 3B; 1224 \pm 132.48; 250–500 μ m: 396

\pm 48.24 and > 500 μ m: 381.6 ± 47 for AY9944; <250 μ m: 1752 ± 18.28 ; 250–500 μ m: 1032 ± 96 and > 500 μ m: 612 ± 84.68 for A-Lova + GGPP). However, similar to what was observed *in vitro*, animals that received A-Lova or GGPP alone showed no enhanced regeneration beyond control levels (Fig. 3Ab and 3Ac). Together these results indicate that *in vivo*, cholesterol inhibition can promote regeneration, however prenylation inhibition was also sufficient to abrogate this positive effect in A-Lova treated animals.

The above presented data indicate that cholesterol inhibition with small molecular drugs promotes axonal regeneration. Because these drugs may have off-target effects, we also exploited siRNA-mediated knockdown of delta-7-sterol reductase (DHCR7) as an alternative approach to abrogate cholesterol biosynthesis (Fig. 4A–D). DHCR7 is the final enzyme of mammalian sterol biosynthesis that converts 7-dehydrocholesterol (7-DHC) to cholesterol. The efficiency of siRNA knock-down was examined following injection in the eye and suggested that DHCR7-siRNA resulted in DHCR7 down-regulation in retinal ganglion cells (Supplementary Fig. 3). To allow quantification of this down regulation, we performed Western blotting on N1E-115 cells transfected with either DHCR7-siRNAs or control siRNAs. This revealed a 2.4-fold reduction in DHCR7 levels by DHCR7-siRNA when compared to control siRNAs (Fig. 4C and D). Intravitreal injection of siRNA can efficiently silence genes in RGCs (Shabanzadeh et al., 2015), therefore we performed optic nerve injury followed by intravitreal siRNA injection on the same day. Three weeks after injury, regeneration was evaluated using GAP-43 staining. DHCR7-siRNA injection significantly promoted axonal regeneration in the optic nerve. Quantification of axon numbers by length showed that DHCR7-siRNA increased the number of regenerating axons by 8.9-fold relative to controls (Fig. 4A, and B; <250 μ m: 1339 ± 114.54 ; 250–500 μ m: 780 ± 68.26 and > 500 μ m: 480 ± 24.08 for DHCR7-siRNA; <250 μ m: 120 ± 26.18 ; 250–500 μ m: 85.74 ± 24.24 and > 500 μ m: 77.14 ± 21.57 for controls). This serves to further confirm a direct role for cholesterol-synthesis inhibition in promoting axonal regeneration following injury.

3.4. Cholesterol synthesis inhibition promotes both RGC- and photoreceptor-survival

In addition to impairing regeneration, the RGMa/Neogenin pathway is also a critical trigger of neuronal death in the injured CNS (Koeberle et al., 2010), and localization of Neogenin in lipid rafts is essential to its pathophysiological roles (Tassew et al., 2014). Following optic nerve injury, we have shown that Neogenin association with lipid rafts triggers RGC death (Tassew et al., 2014). In models for inherited retinal degeneration (Retinitis Pigmentosa) in which photoreceptors progressively undergo cell death, blocking Neogenin function promotes photoreceptor survival (Charish et al., 2020). Here we tested the possibility that cholesterol synthesis inhibition may promote neuronal survival in our models of optic nerve crush and Retinitis Pigmentosa.

First we assessed RGC survival following optic nerve crush. ONCs were performed on rats as before and 3 weeks after injury retinas were collected. RBPMs (Rodriguez et al., 2014) staining or Fluorogold retrograde labelling was performed to visualize surviving RGCs (Fig. 5A

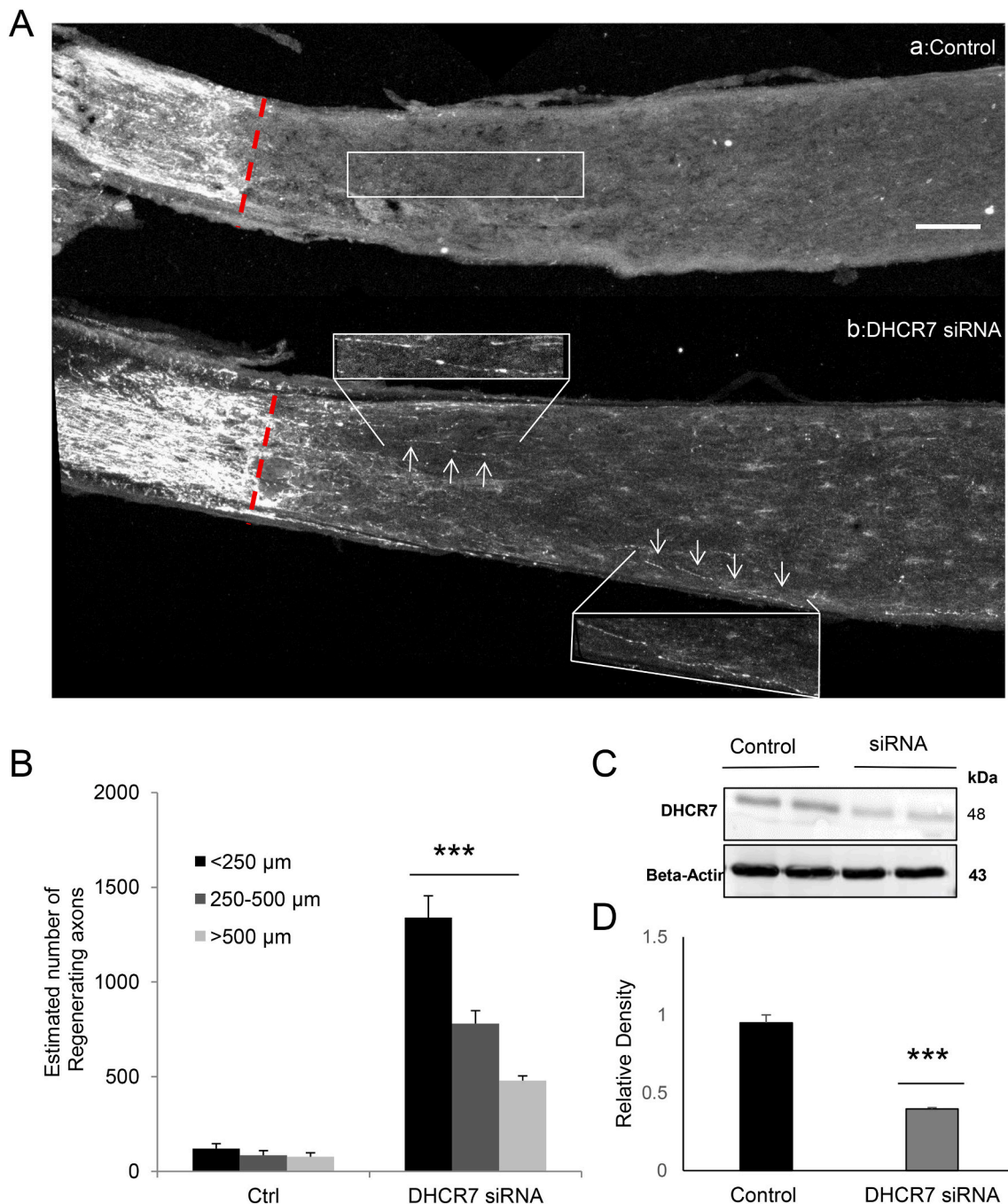


Fig. 4. DHCR7 siRNA promotes axonal regeneration after optic nerve injury.

A, GAP-43 immunostaining in longitudinal sections of optic nerve at 21 days after optic nerve crush. Crush site is indicated by slanted dash line. Arrows demarcate some of the regenerating axons in each section. The retina (not visible) is towards the left-hand side of each image. Nerves that received scrambled siRNA (negative control; $n = 7$) by IO delivery showed minimal axonal regeneration beyond the crush site. 7-Dehydrocholesterol reductase siRNA (DHCR7 siRNA; $n = 7$) increased axonal regeneration into the distal optic nerve after optic nerve crush. **B**, Quantification of the mean number of regenerating axons (\pm SEM) at 21 days following optic nerve crush and treatment with DHCR7 siRNA. The number of axons was quantified in three bins distal to the crush site (0–250 μ m, 250–500 μ m, and > 500 μ m). **C**, Western blots of N1E-115 neuroblastoma cells lysates treated with control siRNA and DHCR7 siRNA. Lysates were probed with anti-DHCR7 and Beta-actin loading controls. **D**, DHCR7 siRNA caused a 2.4 fold reduction in DHCR7 when compared to corresponding control. *** $P < 0.001$ vs. control; scale bar, 200 μ m.

and B, Supplementary Fig. 4A–D). RGC survival was assessed in three different areas (inner, middle, outer) of the retina to reflect regional differences. Intravitreal injection of A-Lova or GGPP on its own did not significantly alter survival when compared to controls. When A-Lova was injected together with GGPP, this resulted in a ~ 3 fold increase in RGC survival, suggesting that in the A-Lova alone treatment condition, a pro-survival effect of cholesterol synthesis inhibition was counteracted by a detrimental effect of GGPP-synthesis inhibition on survival (Fig. 5A

and B, Supplementary Fig. 1 A–D). Injection of AY9944 also resulted in increased RGC survival, supporting the notion that cholesterol-synthesis inhibition leads has a beneficial effect on neuronal survival (Fig. 5A and B).

Our data demonstrate that cholesterol synthesis inhibition promotes both axonal regeneration and RGC-survival. Therefore, we also examined the intra-retinal integrity of RGC axons after optic nerve crush. Rats received optic nerve crush injury followed three weeks later by

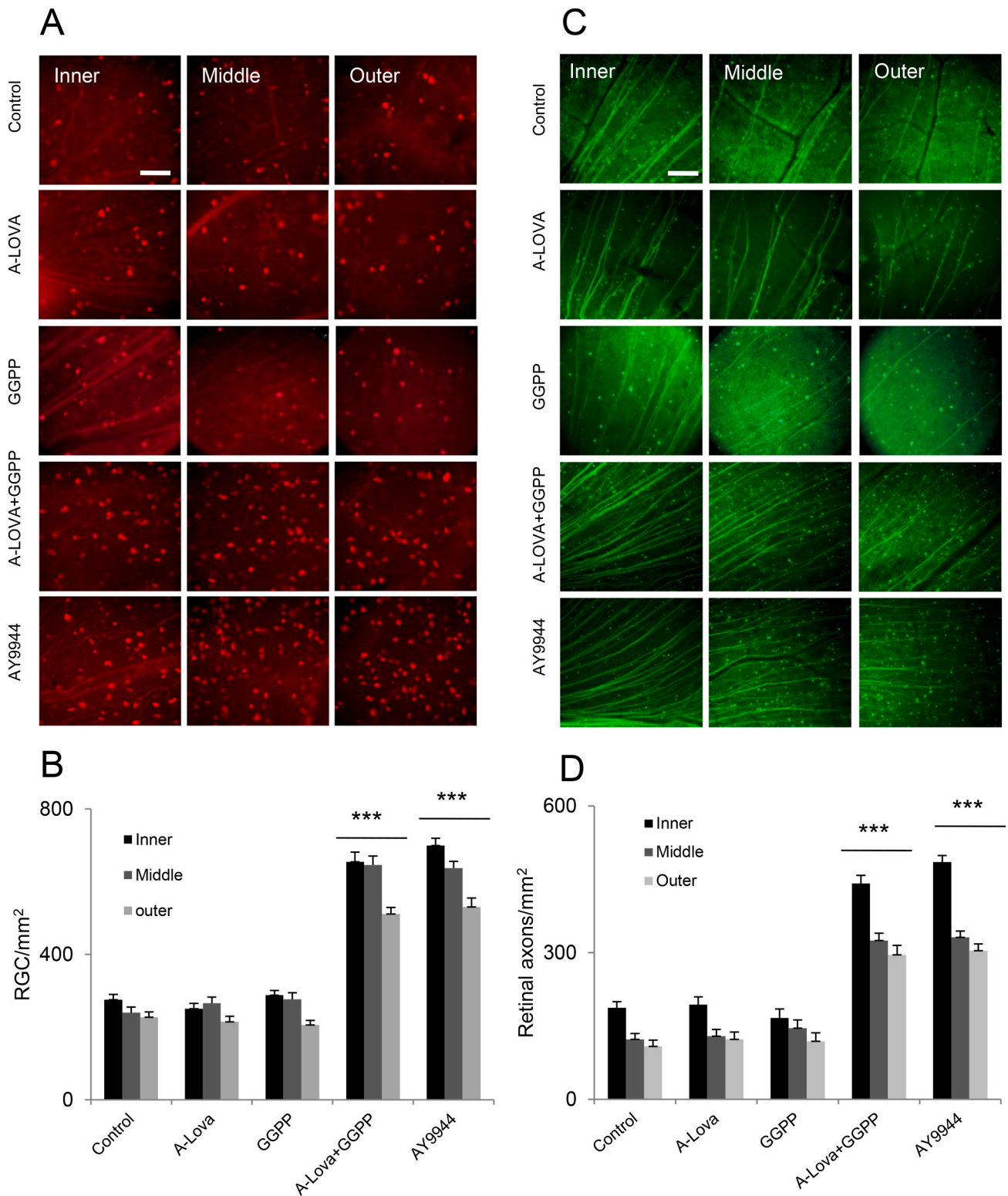
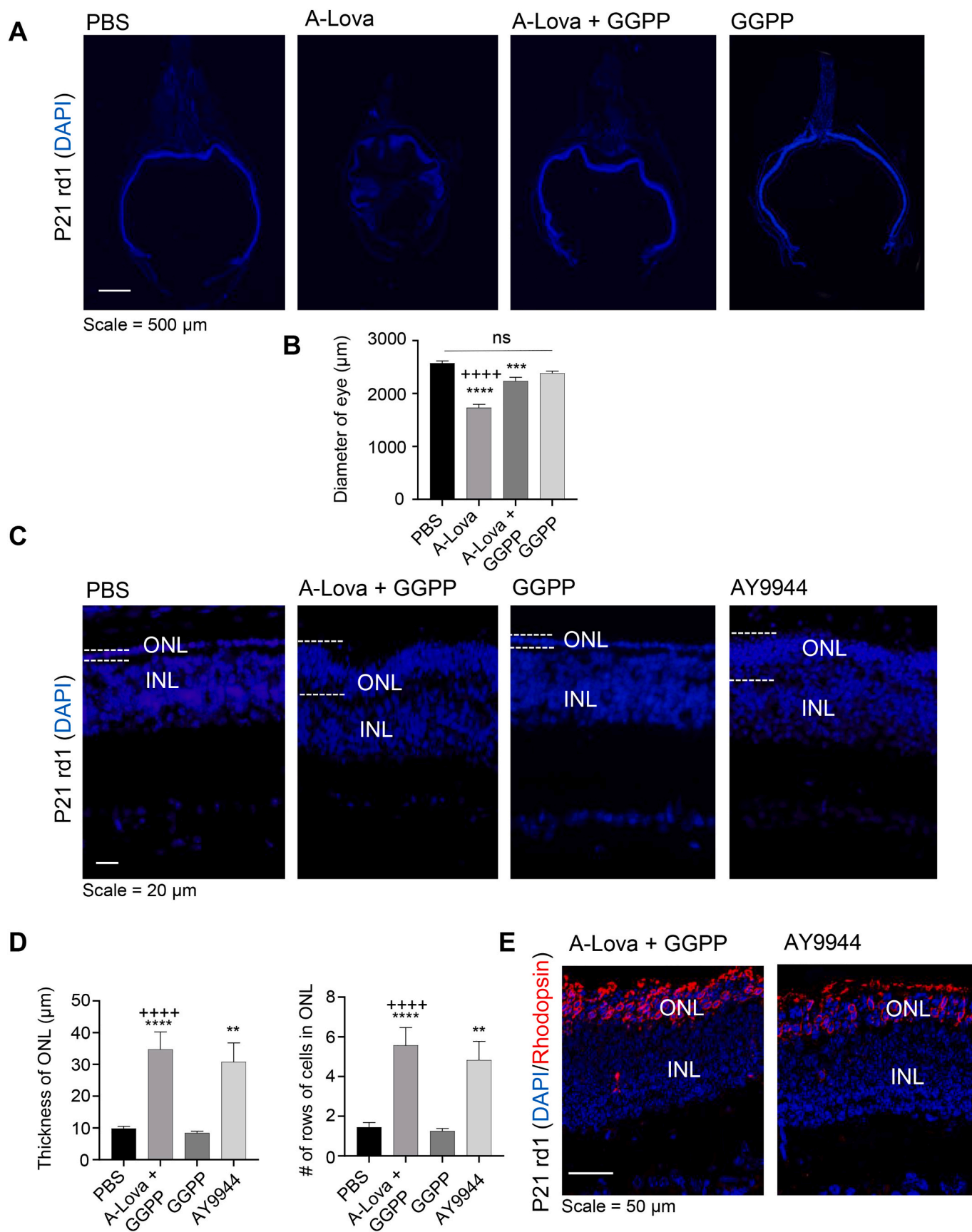


Fig. 5. Cholesterol synthesis inhibition promotes RGC survival and intraretinal axon integrity after optic nerve crush.

A, Images of RBPMs-labeled RGCs at 21 days following optic nerve crush. Images were taken in the inner, mid-periphery (middle), or periphery (outer) of the retina. **B**, Quantification of the density (cells/mm²) of surviving RGCs at 21 days following optic nerve crush, treatment with A-Lova ($n = 7$), GGPP ($n = 6$), A-Lova + GGPP ($n = 7$), and AY9944 ($n = 7$). A-Lova + GGPP and AY9944 led to a significant increase in RGC survival after optic nerve crush. **C**, Fluorescence micrographs of flat-mounted retinas showing FITC-conjugated cholera toxin B (CTB-FITC) labeled axons at 21 days after optic nerve crush. **D**, Quantification of the axon integrity (axons/mm²) of RGCs at 21 days following optic nerve crush and various intraocular (IO) treatment. Control retinas (DMSO, optic nerve crushed, $n = 7$), GGPP ($n = 6$), and A-Lova ($n = 7$) showed similar axonal integrity, whereas A-Lova + GGPP ($n = 7$) and AY9944 ($n = 7$) had significantly higher axon integrity than controls (** $P < 0.001$ relative to control). Axon integrity was grouped by retinal eccentricity (inner, middle, outer) and expressed as mean \pm SEM, Scale bar, 50 μ m.



(caption on next page)

Fig. 6. Inhibiting cholesterol synthesis promotes photoreceptor survival in rd1 mice.

Rd1 eyes were given intravitreal injections at post-natal day (P)9 and P15 of either PBS, A-Lova, A-Lova + GGPP (Geranylgeranyl pyrophosphate), GGPP or AY9944. Eyes were harvested at P21 and cryosectioned. **A**, Nuclear stain (DAPI; blue) of P21 rd1 eyes treated with either PBS, A-Lova, A-Lova + GGPP or GGPP alone. Scale = 500 μ m. **B**, Quantification of data in **A**. The diameter of the eye was measured at the widest point in cryosections from the central retina (i.e. sections containing the optic nerve) ($n = 8$ for each group. PBS vs. A-Lova, **** $p < 0.0001$; A-Lova vs. GGPP, **** $p < 0.0001$; A-Lova + GGPP vs PBS, ***, $p = 0.001$). Data presented as mean \pm SEM. **C**, Representative images of nuclear stain (DAPI; blue) at 400 μ m from the optic disc. Dashed lines indicate the border of the Outer Nuclear Layer (ONL). INL: Inner Nuclear Layer. Scale = 20 μ m. **D**, Quantification of **C**. The thickness and the number of rows of cells in the ONL were measured at 400 μ m from the optic disc in the nasal and temporal quadrant of each eye and averaged. ($n = 8$ for each group; ****, $p < 0.0001$ vs PBS; **, $p < 0.01$ vs PBS; +++, $p < 0.0001$ vs GGPP). Data presented as mean \pm SEM. **E**, Representative images of A-Lova + GGPP and AY9944 treated rd1 eyes at P21 stained for Rhodopsin (red) and a nuclear stain (DAPI; blue), indicating that the cells in the ONL are photoreceptors. Scale = 50 μ m.

intraocular injections of CTB-FITC, an anterograde tracer that allows surveying active protein transport in the axons of neurons. Retinas were flat-mounted 2 d after CTB-FITC injection, and RGC axon integrity was examined in the nerve fiber layer, in the inner, midperiphery, and outer retina (Fig. 5C and D). In control animals, axon bundles appeared thin in the central part of the retina, near the optic disc, where RGC axons turn into the optic nerve (Fig. 5C), and only a low number of projections could be observed in the midperiphery (Fig. 5C) and outer retina (Fig. 5C). The cell bodies of surviving RGCs with intact axons were also visibly labeled with CTB-FITC (Fig. 5C). No obvious change could be observed in retinas treated with A-Lova (Fig. 5C and D). Treatment with A-Lova + GGPP or AY9944 (Fig. 5C and D), resulted in a strong increase of axon integrity throughout the retina, which is consistent with a role of for cholesterol-synthesis inhibition in promoting both cell survival and axonal regeneration. Prenylation inhibition is again suggested to have a negative effect on these parameters. In order to evaluate the effect of cholesterol inhibition on both astroglia and microglia cells, we performed an immunostaining for GFAP (astroglia) and Iba-1 (microglia). Treatments (AY9944, A-Lova, GGPP, A-Lova + GGPP) were performed at injury time and the eyes were collected 5 days after optic nerve injury. None of the treatments induced a change in either GFAP intensity or the number of Iba-1 positive cells (Supplementary Fig. 5). Although this cannot definitely rule out the involvement of astroglia or microglia cells on the treatment effect following injection, this suggests, together with our in vitro data, that regeneration and survival most likely results from a direct effect of our treatments on RGCs.

In order to test the possibility that cholesterol inhibition can also promote the survival of photoreceptor cells during retinal degeneration, rd1 mice were used (Fig. 6A–E). The rd1 (retinal degeneration 1) mouse model is the most extensively studied model of Retinitis Pigmentosa (Han et al., 2013; Kalloniatis et al., 2016). These mice display a very rapid and severe form of retinal degeneration characterized by the rapid loss of rod photoreceptors due to a nonsense mutation in the gene for the beta subunit of rod cGMP PDE6 (Pittler and Baehr, 1991). Rd1 mice were given two intraocular injections of A-Lova, one at P9, corresponding to the onset of rod cell death, and one at P15 (Portera-Cailliau et al., 1994). Eyes were harvested at P21, an age corresponding to when over 90% of rods are gone and the ONL is uniformly reduced to one cell layer thick, with most of the remaining cells being cone photoreceptors (Grimm et al., 2004; Mitton et al., 2014). Following A-Lova intravitreal administration, at P21 we observed obvious negative effects on retinal survival and morphology. There was a significantly reduced eye size coupled with abnormalities such as retinal folds and rosettes in the photoreceptor layer compared to control treated rd1 eyes (Fig. 6A). This is consistent with previous findings indicating that intravitreal A-Lova injection promotes retinal degeneration due to reduced prenylation (Pittler et al., 1995). Here we also observed that A-Lova on its own induced a reduction of eye size, which was significantly improved when A-Lova was combined with GGPP. (Fig. 6A and B). Importantly we also observed a significant promotion in photoreceptor survival in rd1 mice treated with either A-Lova + GGPP or AY9944 when compared to control treated rd1 mice (PBS or GGPP alone; Fig. 6C–E). This indicates that A-Lova promotes adverse retinal effects through prenylation inhibition rather than lowered cholesterol levels, and supports a model in which localized inhibition of neuronal cholesterol synthesis can promote

neuronal survival in cases of neuronal degeneration or injury.

4. Discussion

The data presented here demonstrate novel functions for cholesterol-inhibition following CNS insult or degeneration. We demonstrate that cholesterol inhibition promotes RGC survival following optic nerve injury as well as photoreceptor survival in a model of Retinitis Pigmentosa. We also show that cholesterol inhibition promotes axonal outgrowth on myelin and RGMa, and induces axonal regeneration in vivo. Moreover, activated A-Lova demonstrated two opposing functions on neuronal regeneration/outgrowth: it promotes regeneration and survival by inhibiting cholesterol synthesis while also hampering regeneration through prenylation inhibition. Thus, our data uncover an unappreciated role for cholesterol synthesis in axon regeneration and neuronal survival following CNS injuries.

In addition to their role in modulating Neogenin function (Tassew et al., 2014), there are various indications that lipid rafts may be a critical regulator of axonal regeneration. The Nogo receptor is a GPI-anchored protein and is naturally present in rafts (Fournier et al., 2001). Ephrins-As, which are strong axon-inhibitors, are also GPI-anchored and require oligomerization in rafts to inhibit growing fibers. Therefore, several CNS-inhibitors rely on lipid rafts to prevent regeneration.

In previous studies, we have shown that cholesterol depletion using M β CD promotes axonal regeneration and cell survival in the injured Central Nervous System, with M β CD promoting regeneration and restoration of locomotor functions in the injured spinal cord (Tassew et al., 2014). The same cholesterol-depletion approach also increases regeneration in the injured Peripheral Nervous System, with M β CD accelerating motor and sensory functional recovery following sciatic nerve injury (Rosello-Busquets et al., 2019). It is possible that cholesterol synthesis inhibition is already part of an endogenous mechanism that allows for regeneration following injuries. Unlike the CNS, the Peripheral Nervous System (PNS) has the ability to regenerate its axonal network when injured, and during peripheral nerve regeneration cholesterol synthesis in the nerve is down-regulated (Goodrum, 1990). This fits with our data showing that lower cholesterol-synthesis promotes regeneration and may suggest that our body is already equipped with endogenous cholesterol-modulation strategies to promote regeneration in the periphery.

A large screen for pro-regenerative small molecular drugs identified statins as potential therapeutics capable of accelerating neuronal regeneration in CNS pathologies, and treatment with Cerivastatin specifically was shown to promote axonal regeneration in a model of optic nerve crush (Li et al., 2016). Using in vitro experiments, the authors concluded that this pro-regenerative activity was due to Cerivastatin's effect on prenylation rather than cholesterol synthesis. At first view, this work appears to contradict studies showing that cholesterol depletion enhances neuronal regeneration, however here we reveal that statins can potentially have multiple, and sometimes contradictory, activities axonal growth.

One potential challenge when using drug screening approaches is that screenings may be performed without any prior activation of the compounds present in the library. This may be problematic in the case of

compounds that exist in prodrug forms which may have differing activities from their activated counterparts. Here we found that while the inactive lactone form of Lovastatin (NA-Lova) was sufficient to promote axonal growth on an inhibitory substrate, via a mechanism that may involve reduced prenylation, the active form of Lovastatin (A-lova) could only promote outgrowth/regeneration when prenylation was restored with the addition of GGPP.

The effect of prenylation on outgrowth can vary depending on the molecular and cellular context. As such, altering protein prenylation with statins promotes neurite growth in some systems (Li et al., 2016; Pooler et al., 2006) but decreases it in others (Fan et al., 2001; Kim et al., 2009; Schulz et al., 2004). Statin treatment has been shown to either have no effect on axon elongation in cortical (Fan et al., 2001) or sympathetic neurons (Kim et al., 2009), increase neurite length in hippocampal- and motor –neurons (Li et al., 2016; Pooler et al., 2006), and decrease neurite length in PC12 (Schulz et al., 2004) and sympathetic dendrites (Kim et al., 2009). The reasons behind the different results reported in these studies remain to be fully uncovered, but may involve context specific effects of prenylation. Our data furthermore suggest that i) differences in activation status, ii) conflicting effects of prenylation on axonal growth, and/or iii) the nature of the substrate used to study outgrowth, may together provide some explanation for these opposing results. A better understanding of this duality and the further dissection of statins' pleiotropic effects will be key to harnessing any therapeutic potential of these drugs towards the promotion of neuronal regeneration and survival following CNS injuries. Importantly, here we confirm that inhibiting cholesterol synthesis independent of affecting prenylation is sufficient to promote regeneration.

Funding

This work was supported by the Heart and Stroke Foundation of Canada (Grant number NA7067), The Glaucoma Research Society of Canada, and the Canadian Institutes for Health Research (Grant number MOP106666).

Credit author statement

Alireza P. Shabanzadeh: Performed biochemical, molecular, retinal whole-mount and optic nerve injury/regeneration experiments; Jason Charish: performed Photoreceptor experiment; Nardos G. Tassew, Nahal Farhani,: axonal growth experiments; Andrea J. Mothe: Performed nerve injury experiments; Jinzhou Feng, Xinjue Qin, Shuzo Sugita: Conceptualization and methodology; Thomas Wälchli1, Paulo D. Koerberle: Investigation and supervision; Philippe P. Monnier: Principal investigator.

Declaration of Competing Interest

The authors declare that they have no conflict of interest.

Acknowledgements

We thank Dr. F. Thong for constant support, advice, and discussions. We thank Shirley Chen for performing blinded quantification of axonal growth.

Appendix A. Supplementary data

Supplementary data to this article can be found online at <https://doi.org/10.1016/j.nbd.2021.105259>.

References

- Berry, M., et al., 1996. Peripheral nerve explants grafted into the vitreous body of the eye promote the regeneration of retinal ganglion cell axons severed in the optic nerve. *J. Neurocytol.* 25, 147–170.
- Buss, A., et al., 2009. NG2 and phosphacan are present in the astroglial scar after human traumatic spinal cord injury. *BMC Neurol.* 9, 32.
- Charish, J., et al., 2020. Neogenin neutralization prevents photoreceptor loss in inherited retinal degeneration. *J. Clin. Investig.* 130, 2054–2068.
- Dietschy, J.M., Turley, S.D., 2001. Cholesterol metabolism in the brain. *Curr. Opin. Lipidol.* 12, 105–112.
- Fan, Q.W., et al., 2001. Cholesterol-dependent modulation of tau phosphorylation in cultured neurons. *J. Neurochem.* 76, 391–400.
- Fournier, A.E., et al., 2001. Identification of a receptor mediating Nogo-66 inhibition of axonal regeneration. *Nature.* 409, 341–346.
- Fulcher, J., et al., 2015. Efficacy and safety of LDL-lowering therapy among men and women: meta-analysis of individual data from 174,000 participants in 27 randomised trials. *Lancet.* 385, 1397–1405.
- Gerson, R.J., et al., 1989. Animal safety and toxicology of simvastatin and related hydroxy-methylglutaryl-coenzyme A reductase inhibitors. *Am. J. Med.* 87, 28S–38S.
- Goodrum, J.F., 1990. Cholesterol synthesis is down-regulated during regeneration of peripheral nerve. *J. Neurochem.* 54, 1709–1715.
- Grimm, C., et al., 2004. Constitutive overexpression of human erythropoietin protects the mouse retina against induced but not inherited retinal degeneration. *J. Neurosci.* 24, 5651–5658.
- Guillot, F., et al., 1993. Comparison of fluvastatin and lovastatin blood-brain barrier transfer using in vitro and in vivo methods. *J. Cardiovasc. Pharmacol.* 21, 339–346.
- Han, J., et al., 2013. Review: the history and role of naturally occurring mouse models with Pde6b mutations. *Mol. Vis.* 19, 2579–2589.
- Hata, K., et al., 2006. RGMa inhibition promotes axonal growth and recovery after spinal cord injury. *J. Cell Biol.* 173, 47–58.
- Honda, A., et al., 1998. Regulation of early cholesterol biosynthesis in rat liver: effects of sterols, bile acids, lovastatin, and BM 15.766 on 3-hydroxy-3-methylglutaryl coenzyme A synthase and acetoacetyl coenzyme A thiolase activities. *Hepatology.* 27, 154–159.
- Igarashi, M., et al., 1975. Changes in brain hydrolytic enzyme activities in rats treated with cholesterol biosynthesis inhibitor, AY9944. *Brain Res.* 90, 97–114.
- Kalloniatis, M., et al., 2016. Using the rd1 mouse to understand functional and anatomical retinal remodelling and treatment implications in retinitis pigmentosa: a review. *Exp. Eye Res.* 150, 106–121.
- Keyomarsi, K., et al., 1991. Synchronization of tumor and normal cells from G1 to multiple cell cycles by lovastatin. *Cancer Res.* 51, 3602–3609.
- Kim, W.Y., et al., 2009. Statins decrease dendritic arborization in rat sympathetic neurons by blocking RhoA activation. *J. Neurochem.* 108, 1057–1071.
- Koerberle, P.D., et al., 2010. The repulsive guidance molecule, RGMa, promotes retinal ganglion cell survival in vitro and in vivo. *Neuroscience.* 169, 495–504.
- Kuratomi, S., et al., 2009. The cardiac pacemaker-specific channel Hcn4 is a direct transcriptional target of MEF2. *Cardiovasc. Res.* 83, 682–687.
- Li, H., et al., 2016. Protein Prenylation constitutes an endogenous brake on axonal growth. *Cell Rep.* 16, 545–558.
- Liebscher, T., et al., 2005. Nogo-a antibody improves regeneration and locomotion of spinal cord-injured rats. *Ann. Neurol.* 58, 706–719.
- Magharious, M., et al., 2011a. Quantitative iTRAQ analysis of retinal ganglion cell degeneration after optic nerve crush. *J. Proteome Res.* 10, 3344–3362.
- Magharious, M.M., et al., 2011b. Methods for experimental manipulations after optic nerve transection in the Mammalian CNS. *JoVE* 51, 2261.
- Magharious, M.M., et al., 2011c. Optic nerve transection: a model of adult neuron apoptosis in the central nervous system. *JoVE* 51, 2241.
- McKerracher, L., et al., 1994. Identification of myelin-associated glycoprotein as a major myelin-derived inhibitor of neurite growth. *Neuron.* 13, 805–811.
- Meiri, K.F., et al., 1986. Growth-associated protein, GAP-43, a polypeptide that is induced when neurons extend axons, is a component of growth cones and corresponds to pp46, a major polypeptide of a subcellular fraction enriched in growth cones. *Proc. Natl. Acad. Sci. U. S. A.* 83, 3537–3541.
- Meyer, R.L., et al., 1994. Injury induced expression of growth-associated protein-43 in adult mouse retinal ganglion cells in vitro. *Neuroscience.* 63, 591–602.
- Mitton, K.P., et al., 2014. Different effects of valproic acid on photoreceptor loss in Rd1 and Rd10 retinal degeneration mice. *Mol. Vis.* 20, 1527–1544.
- Molenaar, J.J., et al., 2008. Cyclin D1 and CDK4 activity contribute to the undifferentiated phenotype in neuroblastoma. *Cancer Res.* 68, 2599–2609.
- Monnier, P.P., et al., 2003. The rho/ROCK pathway mediates neurite growth-inhibitory activity associated with the chondroitin sulfate proteoglycans of the CNS glial scar. *Mol. Cell. Neurosci.* 22, 319–330.
- Monnier, P.P., et al., 2011. Involvement of caspase-6 and caspase-8 in neuronal apoptosis and the regenerative failure of injured retinal ganglion cells. *J. Neurosci.* 31, 10494–10505.
- Mothe, A.J., et al., 2017. RGMa inhibition with human monoclonal antibodies promotes regeneration, plasticity and repair, and attenuates neuropathic pain after spinal cord injury. *Sci. Rep.* 7, 10529.
- Muskal, S.M., et al., 2016. Lovastatin lactone may improve irritable bowel syndrome with constipation (IBS-C) by inhibiting enzymes in the archaeal methanogenesis pathway. *F1000Research* 5, 606.
- Ng, W.P., et al., 1996. Human central nervous system myelin inhibits neurite outgrowth. *Brain Res.* 720, 17–24.

- Pittler, S.J., Baehr, W., 1991. Identification of a nonsense mutation in the rod photoreceptor cGMP phosphodiesterase beta-subunit gene of the rd mouse. *Proc. Natl. Acad. Sci. U. S. A.* 88, 8322–8326.
- Pittler, S.J., et al., 1995. In vivo requirement of protein prenylation for maintenance of retinal cytoarchitecture and photoreceptor structure. *J. Cell Biol.* 130, 431–439.
- Pooler, A.M., et al., 2006. The 3-hydroxy-3-methylglutaryl co-enzyme A reductase inhibitor pravastatin enhances neurite outgrowth in hippocampal neurons. *J. Neurochem.* 97, 716–723.
- Portera-Cailliau, C., et al., 1994. Apoptotic photoreceptor cell death in mouse models of retinitis pigmentosa. *Proc. Natl. Acad. Sci. U. S. A.* 91, 974–978.
- Rao, S., et al., 1999. Lovastatin-mediated G1 arrest is through inhibition of the proteasome, independent of hydroxymethyl glutaryl-CoA reductase. *Proc. Natl. Acad. Sci. U. S. A.* 96, 7797–7802.
- Rodriguez, A.R., et al., 2014. The RNA binding protein RBPMS is a selective marker of ganglion cells in the mammalian retina. *J. Comp. Neurol.* 522, 1411–1443.
- Rosello-Busquets, C., et al., 2019. Cholesterol depletion regulates axonal growth and enhances central and peripheral nerve regeneration. *Front. Cell. Neurosci.* 13, 40.
- Sadeghi, M.M., et al., 2000. Simvastatin modulates cytokine-mediated endothelial cell adhesion molecule induction: involvement of an inhibitory G protein. *J. Immunol.* 165, 2712–2718.
- Samuel, F., Hynds, D.L., 2010. RHO GTPase signaling for axon extension: is prenylation important? *Mol. Neurobiol.* 42, 133–142.
- Schaden, H., et al., 1994. GAP-43 immunoreactivity and axon regeneration in retinal ganglion cells of the rat. *J. Neurobiol.* 25, 1570–1578.
- Schulz, J.G., et al., 2004. HMG-CoA reductase inhibition causes neurite loss by interfering with geranylgeranylpyrophosphate synthesis. *J. Neurochem.* 89, 24–32.
- Schwab, M.E., 2004. Nogo and axon regeneration. *Curr. Opin. Neurobiol.* 14, 118–124.
- Schwab, J.M., et al., 2005a. Spinal cord injury-induced lesional expression of the repulsive guidance molecule (RGM). *Eur. J. Neurosci.* 21, 1569–1576.
- Schwab, J.M., et al., 2005b. Central nervous system injury-induced repulsive guidance molecule expression in the adult human brain. *Arch. Neurol.* 62, 1561–1568.
- Shabanzadeh, A.P., et al., 2015. Targeting caspase-6 and caspase-8 to promote neuronal survival following ischemic stroke. *Cell Death Dis.* 6, e1967.
- Shabanzadeh, A.P., et al., 2019. Modifying PTEN recruitment promotes neuron survival, regeneration, and functional recovery after CNS injury. *Cell Death Dis.* 10, 567.
- Tassew, N.G., et al., 2014. Modifying lipid rafts promotes regeneration and functional recovery. *Cell Rep.* 8, 1146–1159.
- Tassew, N.G., et al., 2017. Exosomes mediate mobilization of autocrine Wnt10b to promote axonal regeneration in the injured CNS. *Cell Rep.* 20, 99–111.
- Thomas, S., et al., 2004. Analysis of lipid rafts in T cells. *Mol. Immunol.* 41, 399–409.
- Todd, P.A., Goa, K.L., 1990. Simvastatin. A review of its pharmacological properties and therapeutic potential in hypercholesterolaemia. *Drugs.* 40, 583–607.
- Vreugdenhil, E., et al., 2007. Doublecortin-like, a microtubule-associated protein expressed in radial glia, is crucial for neuronal precursor division and radial process stability. *Eur. J. Neurosci.* 25, 635–648.
- Walther, U., et al., 2016. Lovastatin lactone elicits human lung cancer cell apoptosis via a COX-2/PPARgamma-dependent pathway. *Oncotarget.* 7, 10345–10362.
- Wang, K.C., et al., 2002. Oligodendrocyte-myelin glycoprotein is a Nogo receptor ligand that inhibits neurite outgrowth. *Nature.* 417, 941–944.
- Ward, N.C., et al., 2019. Statin toxicity. *Circ. Res.* 124, 328–350.
- Yu, W., et al., 2004. Segregation of Nogo66 receptors into lipid rafts in rat brain and inhibition of Nogo66 signaling by cholesterol depletion. *FEBS Lett.* 577, 87–92.
- Zhang, G., et al., 2011. Electrical stimulation of olfactory bulb downregulates RGMa expression after ischemia/reperfusion injury in rats. *Brain Res. Bull.* 86, 254–261.